DIFFUSION OF BEAM IONS AT THE TOKAMAK FUSION TEST REACTOR

E. RUSKOV, W.W. HEIDBRINK
University of California,
Irvine, California

R.V. BUDNY
Princeton Plasma Physics Laboratory,
Princeton University,
Princeton, New Jersey

United States of America

ABSTRACT. Various DD and DT plasmas are analysed for effects of fast ion transport with a time dependent, $1\frac{1}{2}$-D transport simulation code (TRANSP). The sensitivity of the simulations to fast ion diffusion modelling is tested against numerous parameters. Strong correlations are found with beam power and plasma stored energy. The neutron emission sensitivity is mostly affected by the fraction of beam–beam neutrons. Wall recycling is essential in interpreting the results for DT plasmas heated with pure deuterium or pure tritium beams. The decay of the 14 MeV neutron emission following a short DT beam pulse implies a small fast ion diffusion coefficient ($D_f < 0.05$ m^2/s). The agreement of the measured neutron emission and diamagnetic flux with the simulations in DT plasmas heated with various numbers of tritium and deuterium beams, and power, implies that $D_f \leq 0.2$ m^2/s.

1. INTRODUCTION

The behaviour of fast ions is a central physics issue for reactor plasmas. The d(t, n)^{4}He reactions are self-sustaining only if the alpha particles are confined long enough to transfer their 3.5 MeV energy to the thermal background plasma. A 1.0–1.5 MeV neutral beam injector to maintain the 22 MA current in the International Thermonuclear Experimental Reactor (ITER) is being considered [1]. Any enhanced fast ion loss will jeopardize the efficiency of this current drive. Finally, a source of auxiliary heating is required to compensate for the transport losses in the preignited plasma. The most likely auxiliary source is the heating in the ion cyclotron range of frequences (ICRF), which generates substantial fast ion populations. Confinement times ≥ 1 s are required for alpha particles in ITER, which sets a limit on the fast ion diffusion coefficient ($D_f < 0.5$ m^2/s) [2]. The spatial concentration of lost fast ions is of particular concern, since it creates hots spots and endangers the machine integrity.

The actual fast ion transport can be diffusive or convective and depends on the velocity and spatial position of the particle. However, it is common to quantify the transport with an effective zero dimensional (0-D) fast ion diffusion coefficient D_f. From the several hundred papers published on fast ions in tokamaks, less than two dozen have quantified this parameter. A recent review [3] surveys the experimental results.

Several groups used 'burnup' measurements to infer the confinement of fusion products. For TFTR supershot plasmas with fast ion slowing down times on electrons $\tau_{se} \sim 1$ s, a 50% reduction in the classically expected tritium burnup fraction was found [4], implying that $D_f \leq 0.1$ m^2/s. Burnup fractions for JET plasmas with $\tau_{se} \geq 2$ s implied similar D_f (0.1–0.3 m^2/s) [5]. Tritium and ^{3}He burnup at DIII-D were simultaneously measured for plasmas with and without MHD activity [6]. While burnup in quiet plasmas was consistent with small anomalous loss ($D_f < 0.1$ m^2/s), for plasmas with strong MHD activity (fishbones, TAE modes) $D_f \geq 1$ m^2/s was implied.

Measurements of escaping DD fusion products (protons and tritons) resulted in a diffusion coefficient for counterpassing MeV ions at TFTR of less than 0.1 m^2/s [2].

The flux of 100 keV protons from a hydrogen minority ICRF heated TFTR plasma was observed with a vertically viewing charge exchange analyser [7]. The radial dependence of the signal implied that $D_f < 0.05$ m^2/s for these trapped ions. At JET, the measured stored energy of tail ions produced by hydrogen minority ICRF heating was compared with the prediction from the Stix model [8]. Their excellent agreement set a limit $D_f < 0.2$ m^2/s.

The first reported value of a fast ion diffusion coefficient ($D_f < 0.5$ m^2/s) was obtained from the absolute magnitude of the 2.5 MeV neutron emission in a PLT plasma heated with ~ 45 keV deuterium beams [9]. More recently, the 2.5 and 14 MeV neutron emission from the partial DT experiments at JET [10] was analysed. No enhanced fast ion loss was required to explain the time evolution and absolute magnitude of the measured signals.

In contrast to the previous work, our study focuses on high power, reactor relevant DT plasmas. We want:

(a) To estimate an upper bound on D_f for these plasmas.
(b) To parametrize the sensitivity of fast ion diffusion modelling with regard to (global) quantities that are easily measurable, such as the total neutron emission and the diamagnetic flux.

In Section 2 we discuss how these two questions are addressed and the selection criteria for the 13 DD and 15 DT analysed plasmas. The measured and the TRANSP predicted neutron emission and diamagnetic flux for the DT plasma set are compared in Section 3. Section 4 discusses the departures of the simulated neutron emission and diamagnetic flux when $D_f > 0$ from their values in the baseline case $D_f = 0$. To support the major result of this study (i.e. $D_f \leq 0.2$ m^2/s for high power DT plasmas), a systematic error analysis of TRANSP simulations for one DT shot is given in the Appendix.

2. TOOLS AND METHODOLOGY

The various complex physical processes in tokamak plasmas require sophisticated computer simulation tools to bring together theoretical models with measured data. One of the most comprehensive such tools is the $1\frac{1}{2}$-D time dependent transport code TRANSP [11–13]. It is routinely used for analysis of plasma discharges at TFTR, PBX-M, JET, ASDEX Upgrade, TEXTOR and Tore Supra. Recently, it was adopted for analysis of DIII-D [14] and Alcator C-Mod plasmas [15].

Throughout this study TRANSP is run in an interpretative mode with standard preparation of the input diagnostics data [16]. Enhanced fast ion transport is modelled with a spatially constant diffusion coefficient. Several values of D_f (0.1, 0.2, 0.5 and 1.0 m^2/s) are used. The predicted neutron emission and diamagnetic flux (DMF) are compared with measurements and with baseline simulations ($D_f = 0$). The MINGL database [17] is used in the search for correlations between the sensitivity of these two parameters to fast ion diffusion modelling, and other plasma parameters.

Since our conclusions about fast ion transport in TFTR plasmas are based on the agreement of the predicted neutron emission and DMF with measurements, knowledge of the uncertainities of these measurements is essential.

2.1. Neutron emission and diamagnetic flux measurement uncertainties

Three ^{235}U and four ^{238}U fission chambers are used as basic neutron emission diagnostics at TFTR [18–23]. The two 1.3 g moderated ^{235}U detectors (designated as NE-1 and NE-2) are the most sensitive and they have been repeatedly absolutely calibrated with in situ neutron sources, including ^{252}Cf point sources [18, 21], and DD and DT neutron generators [20, 24]. In count rate mode they measure source strengths up to 4×10^{14} n/s, with an uncertainty (one σ) of $\pm 13\%$ [21, 24]. The major source of this uncertainty (8–12%) is the correction for energy sensitivity if a ^{252}Cf source is used, or the uncertainty of the total neutron generator output [22].

Campbelling and current mode operation of the detectors NE-1 and NE-2 is necessary for measurement of stronger neutron emission (up to $> 10^{17}$ n/s [21]), and for cross-calibration of the less sensitive fission detectors. In September 1994 two silicon diode detectors were installed [25], and they facilitated the fission detector cross-calibration for DT plasmas [23]. The silicon diode detectors register 14 MeV neutrons only, and they are cross-calibrated to the TFTR neutron activation system, which has $\pm 10\%$ uncertainity [26].

The absolute accuracy of the neutron measurements during DT operations, determined by an uncertainty weighted mean of independently calibrated detector systems, is estimated [23] to be about $\pm 7\%$. The uncertainty (one σ) of the neutron measurements during DD operations was estimated [22] to be $\pm 15\%$. We analyse both DD and DT plasmas, thus we assume a conservative value of $\pm 15\%$ (one σ) neutron emission uncertainty throughout this study.

Two diamagnetic loops [27] measure the displaced magnetic flux from the plasma. They provide indirect measurement of the perpendicular plasma pressure and analysis of the diamagnetic flux, and the equilibrium magnetic field determines the total stored plasma energy [28]. Instead of comparing measured and TRANSP predicted plasma stored energies, we

choose to compare the directly measured quantity (the diamagnetic flux) and the corresponding TRANSP prediction.

For normal TFTR discharge conditions (toroidal field current in the range −56 to −73 kA, plasma currents in the range 0.5 to 2.5 MA), the random (noise) component of the DMF uncertainty is small (~ 0.2 mWb). However, the systematic uncertainty due to uncompensated toroidal and poloidal field fluxes is substantial, and its maximum level is estimated to be 1 mWb. The calibration uncertainty is ~0.25% of the flux itself. Therefore, the overall absolute uncertainty of the DMF measurements, for normal discharge conditions, is estimated to be ±1.2 mWb [29]. This is the value we use in our study.

2.2. Selection criteria

We are most interested in high power DT plasmas, with various fractions of tritium and deuterium beam fuelling. To see if they behave differently with regard to fast ion diffusion modelling, we include several kinds of DD plasmas in our analysis.

The first selection criterion for the shot set is the availability of a baseline ($D_f = 0$) TRANSP simulation. In general, cases with good agreement between the measured and simulated neutron emission and diamagnetic flux are chosen. A few cases that are likely candidates for fast ion loss (low current and/or large plasma) and have overestimated values of these parameters are included (diffusion tends to lower them). To provide material for a study (in preparation) of spatially variable fast ion diffusion, plasmas with spatial neutron emission measurements [30] are preferred.

A total of 15 DT plasmas are analysed. They include: the first trace tritium discharge (No. 72 613); another trace tritium discharge with 0.2% T in eight beam lines (No. 72 635);99a 50 ms, 23.5 MW beam pulse with deuterium and tritium beams (No. 73 253); DT plasmas with beam power in the range 12–30 MW and tritium beam fractions in the range 0.10–0.64; two plasmas heated with tritium beams only, and one with deuterium beams only. Their common parameters are: $R = 2.52$ m, $a = 0.87$ m, $I = 1.8$ or 2 MA, except for one likely candidate for stochastic ripple transport, which has $R = 2.61$ m and $a = 0.96$ m (No. 74 652). All but two of the DT shots are from the December 1993 DT campaign.

Supershots [31] are the basic type of DD plasmas considered, with beam power in the range 12–30 MW. Two L mode plasmas, two high β_p supershots and a supershot with 5 MW of ICRF heating are included for comparison purposes. The DD list is completed with a large ($a = 0.96$ m, $R = 2.61$ m), low current (0.9 MA) plasma heated with 13 MW of beam power (No. 67 241), as a plasma likely to exhibit stochastic ripple diffusion of beam ions.

3. COMPARISON WITH MEASUREMENTS

3.1. DT beam pulse

We start with analysis of a 50 ms, 23.5 MW beam pulse with three tritium and seven deuterium beams (No. 73 253). Previous experiments proved the value of such short pulses in analysing the core transport of beam ions. For example, the time evolution of neutron and charge exchange signals from a low density ohmic TFTR plasma, into which a 20 ms, 12 MW deuterium beam pulse was injected, showed little ($D_f \sim 0.1$ m^2/s at $r/a \simeq 0.5$) or no anomalous beam ion diffusion at all ($D_f \ll 0.1$ m^2/s at the plasma centre) [32].

Because the DT fusion cross-sections is two orders of magnitude larger than the DD cross-section ($E_{CM} \sim$ 100 keV) the total neutron emission is dominated by 14 MeV neutrons. These neutrons are measured with a silicon diode detector [25] which, at the time of this experiment, had a temporal resolution of 5 ms (additional CAMAC memory was installed in May 1994 and the resolution increased to 1 ms).

The measured 14 MeV neutron emission and the corresponding TRANSP predictions for $D_f = 0$, 0.05, 0.1, 0.2, 0.5 and 1.0 m^2/s are shown on Fig. 1(a). Owing to the large difference in the predicted slowing down times, the conclusion that $D_f < 0.05$ m^2/s is straightforward. We confirmed this conclusion with several $D_f = 0.05$ m^2/s simulations with perturbed input data. Perturbations that were likely to affect the neutron emission the most (tests Nos 3, 5, 6 and 16 in Table II) were chosen.

The time evolution of the ion temperature was not measured in this discharge, but fortunately the conclusions are insensitive to the assumed value of T_i (thermonuclear reactions make a minor contribution to the neutron emission). In the modelling, T_i was found by assuming a thermal diffusivity $\chi_i = a\chi_{neo}$, with $a = 3$. Simulations with a neoclassical multiplier $a = 1$, 2, 5, 10, or with the assumption $\chi_i = \chi_e$ do not alter the conclusion that $D_f < 0.05$ m^2/s in this discharge. It was also necessary to include sawtooth modelling in the simulation (without sawteeth, $q(0)$ dropped from 0.9 to 0.4).

The relative importance of beam–beam, beam–target and thermonuclear reactions is shown in

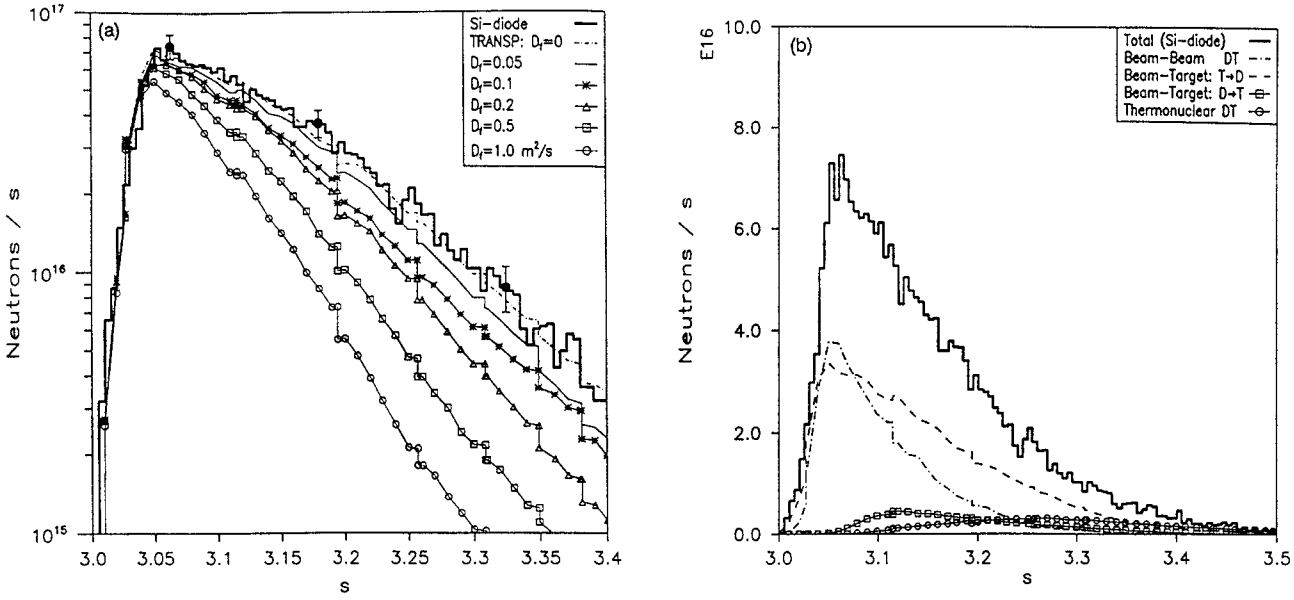

FIG. 1. (a) 14 MeV neutron emission from a DT pulse experiment (No. 73 253), measured with silicon diodes, and TRANSP predictions for various values of the fast ion diffusion coefficient. The error bars include the errors from the counting statistics and the uncertainty from the cross-calibration to the TFTR neutron activation system. (b) 14 MeV neutron emission measured with silicon diodes and TRANSP breakdown into its constituent parts ($D_f = 0$).

Fig. 1(b). At their peak values, half of the emission originates from beam–beam DT reactions, slightly less from tritum beam ions fusing with thermal deuterium, and only a few per cent from deuterium beam ions fusing with thermal tritium, or from thermal DT reactions. Since the beam–beam reactions depend both on deuterium beam and tritium beam ion densities, they decay the fastest, particularly if there is enhanced radial transport. Comparison of the simulations indicates that most of the 14 MeV neutrons in the 3.15–3.30 s interval are from tritium beam ions fusing with thermal deuterium. Therefore, the neutron decay rates in Fig. 1(a) are directly related to the confinement of tritium beam ions.

3.2. Plasmas heated with DT beams

Eight plasmas heated with beams in the range 12–30 MW, and T/D beam fractions in the range 0.10–0.64 are studied for effects of beam ion diffusion. On the low power end is a shot with $P_{nbi} = 12.5$ MW (one tritium and four deuterium beams, No. 73 306) and on the high power end is the record fusion power shot [33] with $P_{nbi} = 30$ MW (seven tritium and four deuterium beams, No. 73 268). The measured and TRANSP simulated total neutron emission and diamagnetic flux for these two shots are shown in Figs 2(a–d). All the data are consistent with zero beam ion diffusion.

The difference in departure of the calculated values, for simulations with non-zero fast ion diffusion, from the corresponding baseline ($D_f = 0$) values is evident. While the low power DT shot shows a strong sensitivity of simulated neutrons to fast ion diffusion (from Fig. 2(a), $D_f \leq 0.1$ m^2/s), and a somewhat weaker sensitivity of the simulated diamagnetic flux (from Fig. 2(b), $D_f \leq 0.2$ m^2/s), the high power discharge has opposite characteristics: the neutrons are quite insensitive (the $D_f = 0.5$ m^2/s case is well within the error bar, Fig. 2(c)) and the diamagnetic flux is quite sensitive to fast ion diffusion modelling (from Fig. 2(d), $D_f < 0.1$ m^2/s). The physical dependences that account for these differences are addressed in Section 4.

To quantify these observations, we define

$$\Delta_{df\_m} = |DMF_{TR} - DMF_m| \quad (1)$$

where DMF_m (DMF_{TR}) is the measured (TRANSP predicted) diamagnetic flux averaged over 200–400 ms (depending on the plasma discharge) around the time of peak stored energy. For the neutrons, we define

$$\delta_{neu\_m} = \frac{|S_{TR} - S_m|}{S_m} \quad (2)$$

where S_m is the peak measured neutron emission and S_{TR} is the peak TRANSP predicted value.

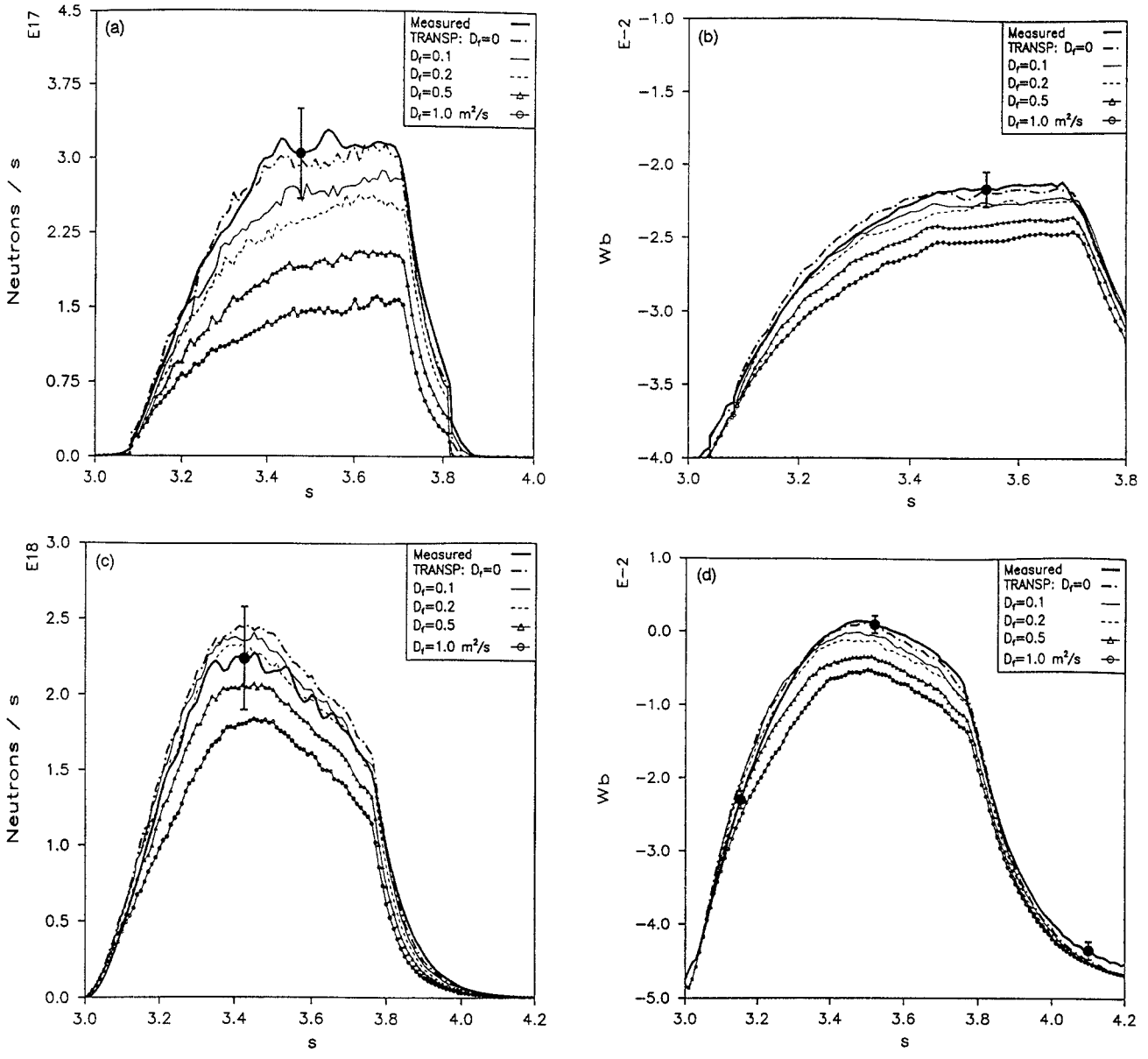

FIG. 2. Measured and TRANSP predicted total neutrons (a) and diamagnetic flux (b) from a low power DT shot (No. 73306). Measured and TRANSP predicted total neutrons (c) and diamagnetic flux (d) from a high power DT shot (No. 73268). The error bars are: 15% for the neutron emission and 1.2 mWb for the diamagnetic flux.

The quality of agreement between simulation and measurement cannot be judged on the basis of these two numbers only; the temporal evolution has to be taken into account as well. Since we choose baseline simulations that are in good agreement with the measured neutrons and diamagnetic flux (both in peak value and shape), and the fast ion diffusion modelling monotonically decreases the baseline values (for exceptions, see Section 4.3), the (δ_{neu_m}, Δ_{df_m}) pairs represent the departure from measurement well.

A (δ_{neu_m}, Δ_{df_m}) measurement comparison map (Fig. 3) summarizes our findings about plasmas heated with deuterium and tritium beams. Points that lie within the box in Fig. 3 are consistent with neutron and DMF measurements (within experimental errors). The obvious feature of the map is that increasing D_f causes the (δ_{neu_m}, Δ_{df_m}) points to 'run away' from the box defining the boundaries of acceptable simulations. In other words, as D_f increases, there is a simultaneous increase in the discrepancy between the

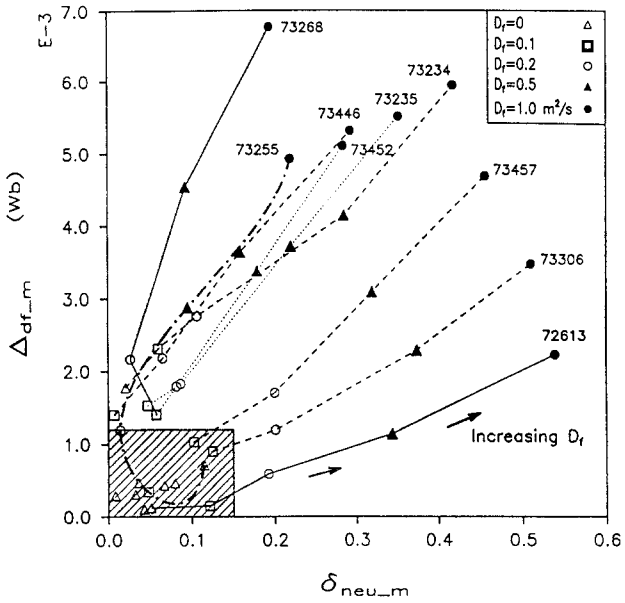

FIG. 3. Map showing the discrepancy between simulation and measurement for the diamagnetic flux (y axis) and total neutron emission (x axis), for a set of nine DT discharges. The line segments connect various D_f simulations of the same shot. The number at the end of a segment identifies the shot. The shaded box defines boundaries of simulations within the accepted error bars.

measured neutron and DMF values and the TRANSP simulations. This confirms that high values of D_f are incompatible with the measurements. While some of the simulations with $D_f = 0.1$ m^2/s stay within the box, for $D_f \geq 0.2$ m^2/s all escape. Therefore, an upper limit on the fast ion diffusion coefficient can be set for these DT plasmas: $D_f \leq 0.2$ m^2/s.

Shot 73 234 has the lowest (0.1) ratio of T/D beams and the baseline DMF prediction is somewhat poorer. Nevertheless, the general features of its trajectory remain the same.

The first trace tritium shot (six deuterium beam lines, one with 2% tritium; $P_{NBI} = 12$ MW, No. 72 613) is included in the set of eight DT shots because its neutron emission is not affected by tritium wall recycling, thus making it a member of a group of discharges with neutron emission relatively independent of this process. The δ_{neu_m} sensitivity of shot 72 613 is similar to the sensitivity to shot 73 306, but its Δ_{df_m} sensitivity is lower because the stored energy is lower (Section 4.1).

As tritium accumulated in the vessel walls, subsequent trace tritium discharges showed less δ_{neu_m} sensitivity. This agrees with the observations from the extreme cases of DT plasmas heated with pure tritium or pure deuterium beams (Section 4.3).

Detailed systematic error analysis for one DT shot is undertaken in the Appendix. We want to check how the choice of physics models, and the errors in the input data affect the established upper bound on D_f. The results from this analysis confirm that $D_f \leq 0.2$ m^2/s.

In the whole set of 28 DD and DT plasmas analysed, we identified two cases that exhibit enhanced beam ion transport. Both of these have large major and minor radii ($R = 2.61$ m, $a = 0.96$ m). Particularly high losses are observed in a low current DD discharge ($I = 0.9$ MA, $P_{NBI} = 13.5$ MW). Stochastic ripple loss is the probable mechanism behind the enhanced beam ion transport and a detailed study of this subject is in preparation.

4. SENSITIVITY OF TRANSP SIMULATIONS TO FAST ION DIFFUSION MODELLING

The interpretation of TFTR experiments relies heavily on TRANSP simulations. Attempts to establish an upper limit on a possible fast ion loss, quantified with D_f, faces the question of how much these simulations are sensitive to fast ion diffusion modelling. On the other hand, knowledge of what influences that sensitivity is useful for designing experiments dedicated to fast ion transport studies.

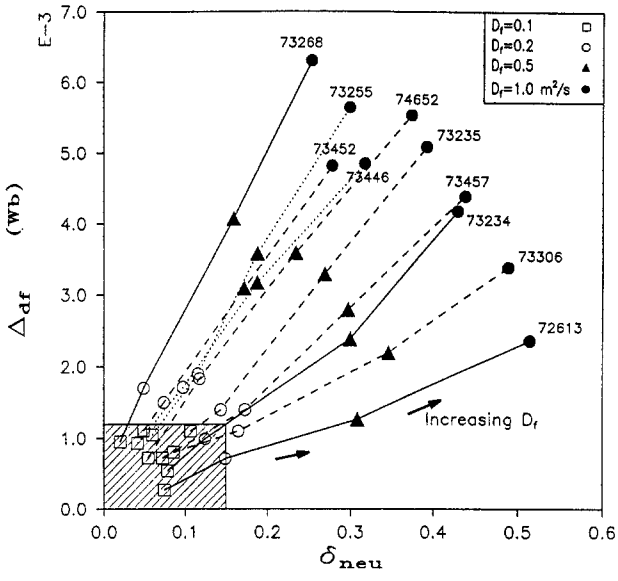

FIG. 4. Sensitivity of TRANSP simulated diamagnetic flux (y axis) and total neutron emission (x axis) to fast ion diffusion modelling. Shots from Fig. 3 and shot No. 74 652 are presented. The line segments connect various D_f simulations of the same shot. The number at the end of a segment identifies the shot. The shaded box is for comparison purposes with Fig. 3.

In Section 3, we compared the simulated values to the measured values and defined parameters Δ_{df_m} and δ_{neu_m} to quantify the agreement with experiment. For a sensitivity study, it is more convenient to compare the simulated values to the baseline $D_f = 0$ simulation, since this makes the results independent of experimental errors. We are mostly interested in the total neutron emission and diamagnetic flux, so we define

$$\Delta_{df} = |\mathrm{DMF}_{TR} - \mathrm{DMF}_{TR\_0}| \quad (3)$$

and

$$\delta_{neu} = \frac{|S_{TR} - S_{TR\_0}|}{S_{TR\_0}} \quad (4)$$

where DMF_{TR_0} and S_{TR_0} are the baseline DMF and neutron emission predictions, and DMF_{TR} and S_{TR} are the predictions for $D_f > 0$.

The (δ_{neu}, Δ_{df}) sensitivity map for the DT shot set is shown in Fig. 4. The difference between Fig. 4 and Fig. 3 is that, in Fig. 4, the simulations are compared with the baseline simulation while, in Fig. 3, the simulations are compared with experiment. By definition, all $D_f = 0$ map points in Fig. 4 appear at the origin. With few exceptions, map points that belong to the same shot move along a straight line. The similarity between Figs 4 and 3 is a testament to the good agreement between baseline simulations and measurements. If the agreement with experiment was perfect, the two maps would be identical.

The DD set produced a similar sensitivity map, with two exceptions: a 0.6 MA high β_p plasma (No. 52 328) and a 1.15 MA small supershot plasma (R = 2.26 m, a = 0.61 m) heated with P_{NBI} = 10 MW (No. 53 934). For both of these discharges, the predicted DMF was extremely insensitive to fast ion diffusion modelling, resulting in horizontal map lines. However, the baseline DD simulations are of uneven agreement with measurements and their (δ_{neu_m}, Δ_{df_m}) measurement comparison map looks quite complicated.

4.1. Diamagnetic flux sensitivity

To understand the dependence of the neutron emission and DMF on fast ion diffusion, basic plasma parameters and numerous parameters from TRANSP simulations are entered into the MINGL database [17]. To obtain better resolution, the Δ_{df} and δ_{neu} departures of the D_f = 1.0 m^2/s simulations are considered in this and the following subsections. If D_f = 0.5 m^2/s simulations are considered instead, the inferred correlations remain the same. The simulations with

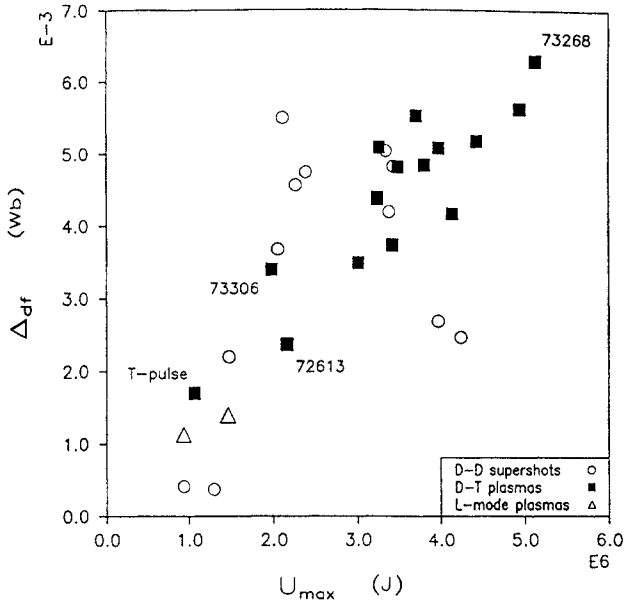

FIG. 5. Correlation between the sensitivity of diamagnetic flux and TRANSP calculated peak total plasma stored energy. The full set of DD and DT discharges is presented. The sensitivity is defined as the absolute difference between the D_f = 1.0 m^2/s and D_f = 0 simulations (Eq. (3)).

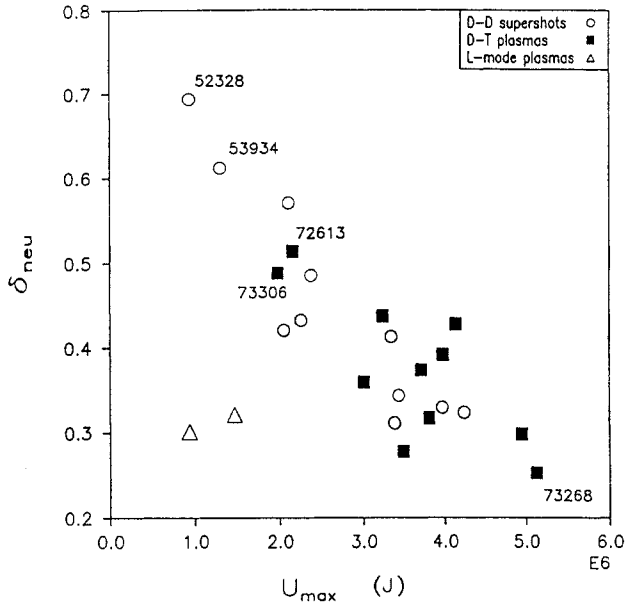

FIG. 6. Correlation between neutron emission sensitivity and TRANSP calculated peak total plasma stored energy. The tritium beam pulse (No. 73 253), a plasma fuelled with pure deuterium beams (No. 73 449) and two plasmas (Nos 73 450, 77 269) fuelled with pure tritium beams are excluded from the presented set. The sensitivity is defined as the relative difference between the D_f = 1.0 m^2/s and D_f = 0 simulations (Eq. (4)).

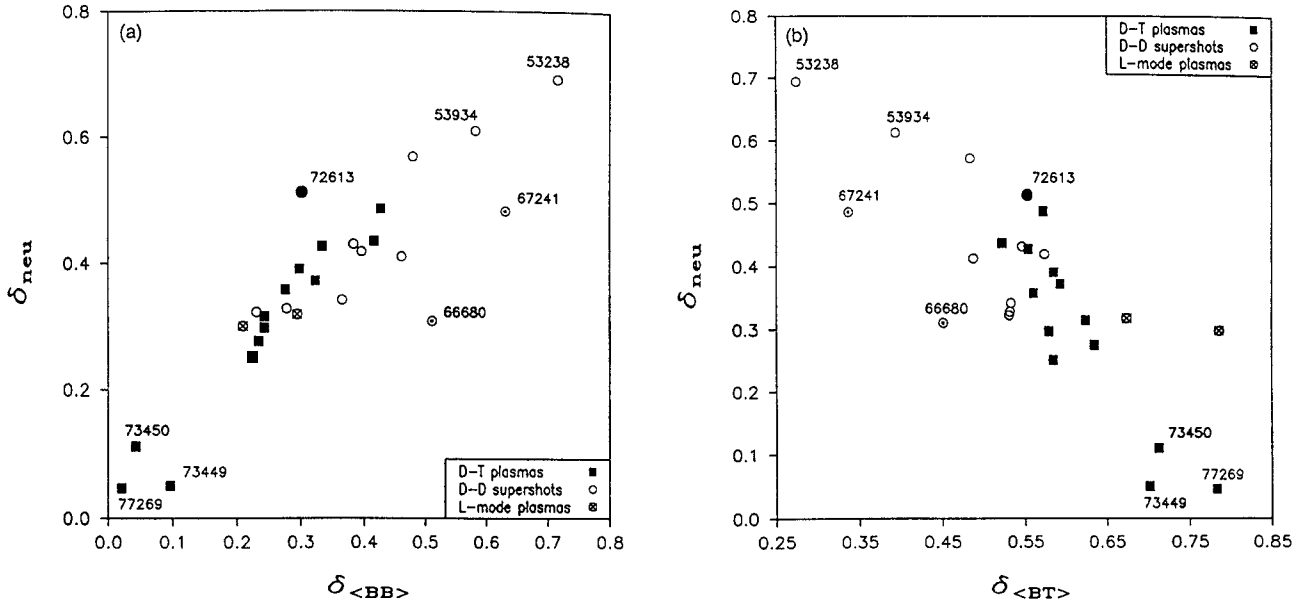

FIG. 7. (a) Correlation between neutron emission sensitivity and TRANSP calculated beam–beam neutron emission, time averaged over the beam duration. (b) Correlation between neutron emission sensitivity and TRANSP calculated beam–target neutron emission, time averaged over the beam duration. Only the tritium beam pulse is omitted from the full set of analysed plasmas: •, first trace tritium shot (No. 72 613); ⊙, lower supershot with $P_{NBI} = 18$ MW and $P_{ICRF} = 4.5$ MW (No. 66 680), upper ripple loss shot (No. 67 241).

D_f = 0.1 and 0.2 m^2/s are not very useful for sensitivity studies, because the departures are small and the scatter is pronounced.

The correlation between the diamagnetic flux sensitivity and the TRANSP calculated peak plasma stored energy, for the full set of DD and DT discharges, is shown in Fig. 5. A particularly strong correlation exists for the set of DT discharges. At the low end is the tritium beam pulse (which is essentially an ohmic plasma), and at the high end is the most powerful discharge in the set (No. 73 268). The beam ion energy content for all DT shots is ~50% and the larger the perpendicular component is, the more sensitive the DMF is. The total plasma stored energy increases with increasing beam power, thus the plot for DMF sensitivity versus beam power is quite similar to Fig. 5.

4.2. Neutron emission sensitivity

The correlation between neutron emission and plasma stored energy, is opposite from the DMF case, Fig. 6. This was already observed (Fig. 2) in Section 3.2, since plasma stored energy is proportional to beam power.

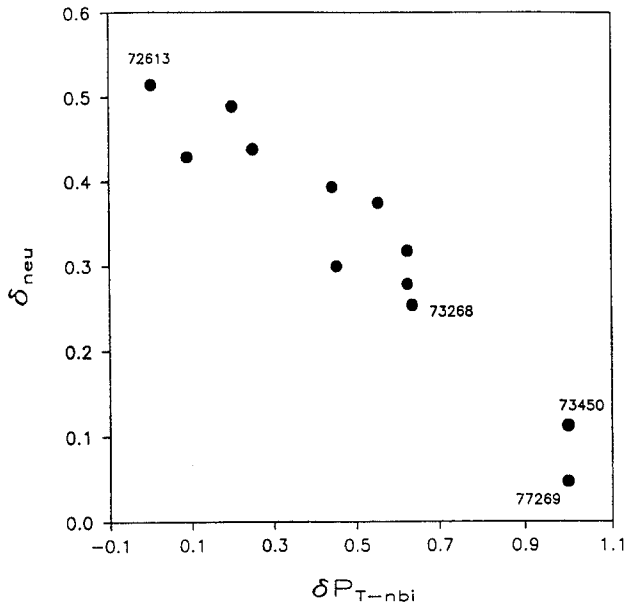

FIG. 8. Correlation between neutron emission sensitivity and fraction of tritium beams lines (each beam line delivers ~ 2.5 MW power). Shot No. 72 613 has 0.2% trace tritium in one of its six beam lines. Plasmas Nos 73 450 and 77 269 are fuelled with pure tritium beams.

A particularly strong correlation in the full plasma set is found between the neutron emission and the fraction of its beam–beam component, time averaged over the beam duration, Fig. 7(a). The existence of such correlation is obvious, since there is a quadratic dependence between beam–beam neutron production and the beam ion density. However, the inverse dependence on the beam–target neutron fraction, Fig. 7(b), is counterintuitive. The larger the fraction of beam–target neutrons, the less sensitive the neutron emission is. The same holds for the thermal neutron fraction, but this again is an expected result.

In the course of our database analysis we tried to correlate the neutron sensitivity with the neutron type fractions calculated at the time when the beams are turned off, and with the time average (over the beam duration) of neutron type fractions within $(a/4)$ the plasma centre. Both trials resulted in more scatter, indicating that the entire history of the whole plasma is important in establishing the sensitivity of the neutron emission. This confirms the advantage of time dependent codes, such as TRANSP, in seeking correlations between various plasma parameters.

Another strong relationship was found for the DT subset: neutron sensitivity decreases as the fraction of tritium beams increases (Fig. 8). This observation is explained in the following subsection.

We investigated the sensitivity of two other parameters to beam ion diffusion: the plasma surface voltage, and the neutron decay rate, after the beams are turned off. Unfortunately, the surface voltage is completely insensitive to beam ion diffusion modelling, and the neutron decay rate is sensitive only in plasmas with large beam–beam neutron fraction.

4.3. Neutron emission sensitivity in DT plasmas heated with pure deuterium or pure tritium beams

The importance of wall recycling was recognized previously [34]. While beam fuelling dominates the inner half of supershot plasmas, wall recycling dominates the outer half, and overall, supplies most of the deuterium ions.

The outgassing fuelling mechanism has dramatic consequences for the neutron emission analysis of DT plasmas heated with pure deuterium or pure tritium beams. Contrary to all of the other conditions, the TRANSP predicted neutron emission does not change even for high values of D_f (Fig. 9(a)).

A closer look at the components of the neutron emission (Table I) reveals that the dominant part is the beam-target neutrons (~70%), and that they are not affected by diffusion of beam ions. The explanation is simple: for single hydrogenic type beams (tritium only; or deuterium only), the walls act as a huge supply of hydrogenic fuel for the other kind (deuterium; or tritium). The 2 orders of magnitude difference between the TT (or DD) and DT cross-sections makes the beam–target reactions dominant. When the fast ion diffusion model is turned on, beam ions are removed from the plasma core and, owing to quasi-neutrality, thermal ions fill their place. Both deuterium and tritium thermal ions move in, but the complementary type (i.e. thermal deuterium for tritium beams, and vice versa) is responsible for compensating the loss (due to removal of beam ions) of beam target neutrons.

TABLE I. COMPONENTS OF NEUTRON EMISSION
(Peak values of the neutron types are given, so their sum might exceed 100%.)

Shot number	Beam-target neutron fraction (%)	Thermal neutron fraction (%)	Beam-beam neutron fraction (%)	T/D beam lines	P_{NBI} (MW)
73 449	69	23	8	0/8	20
73 450	64	33	5	8/0	23
73 457	59	10	38	2/6	21
77 269	70	28	2	5/0	15

The increased levels of thermal deuterium and tritium ions in the inner, hot plasma regions, where the reactivity is higher, result in as much as a 40% increase in the thermal neutron emission for the $D_f = 1.0\ m^2/s$ case (Fig. 9(b)).

Comparison of tritium (Fig. 9(c)) and deuterium (Fig. 9(d)) density profiles in the middle of the beam interval confirms the above picture. While there is little change in deuterium profiles, the tritium profiles increase uniformly along the entire plasma. The $n_T(0)$ density for the $D_f = 1.0\ m^2/s$ case is twice as large as the baseline density.

These results were confirmed with another case of pure tritium beam fuelling (No. 73 450). An interchanged role of deuterium and tritium was observed in a deuterium beam fuelled plasma (No. 73 449). Although the tritium density was about 2 orders of magnitude less than the deuterium density, it was behaving very much as in Fig. 9(d). The deuterium density profile remained constant.

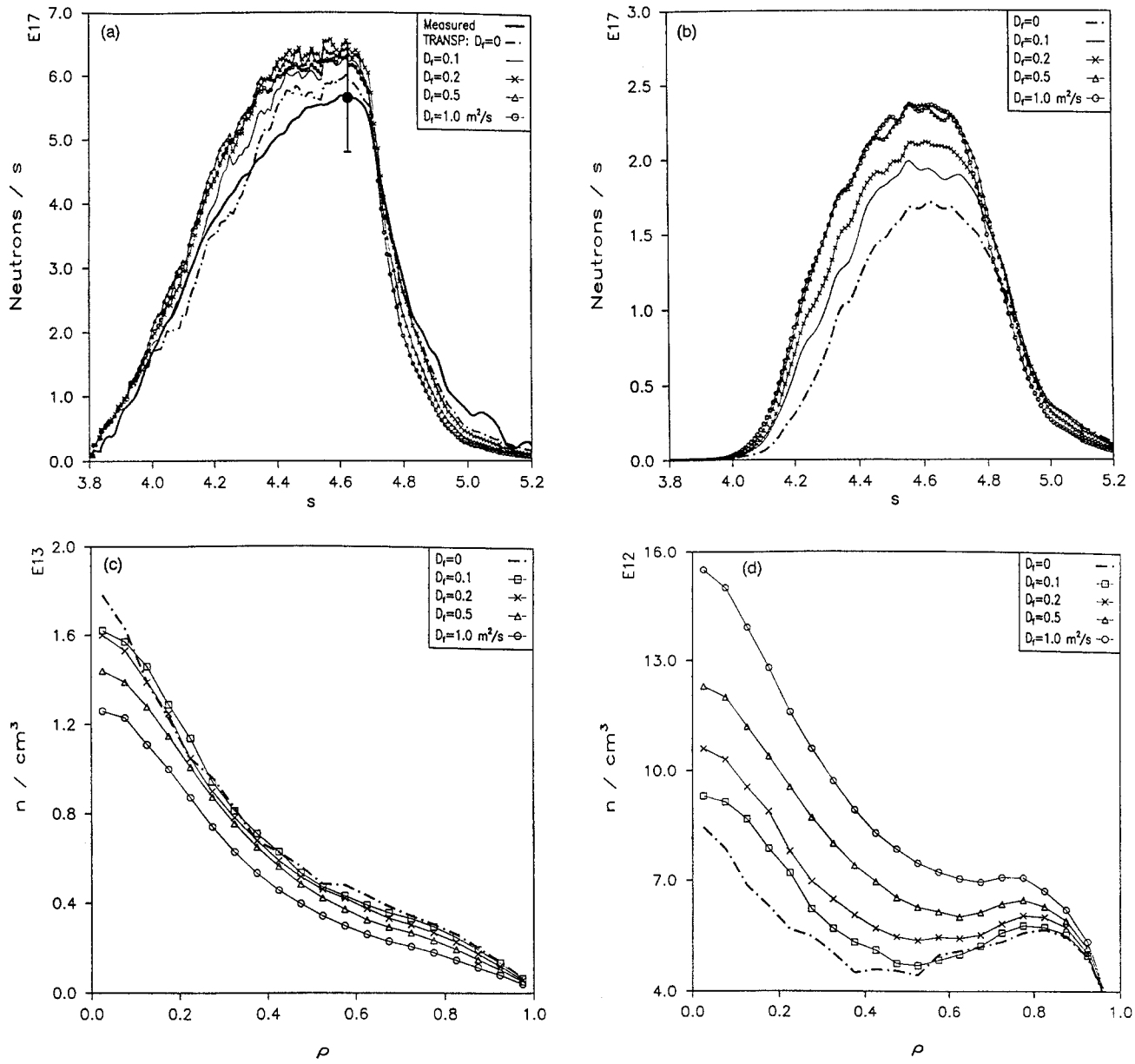

FIG. 9. Influence of deuterium wall recycling on a DT plasma heated with pure tritium beams, P_{NBI} = 15 MW (No. 77269): (a) total neutron emission, (b) thermal neutron emission, (c) tritium profiles in the middle of the beam interval, (d) deuterium profiles in the middle of the beam interval.

A (δ_{neu}, Δ_{df}) sensitivity map summarizes these findings, Fig. 10. The peak neutron emission excursions are within 5%, the TRANSP Monte Carlo noise level. The diamagnetic flux sensitivity is normal, as discussed in Section 4.1.

Neutron emission in plasmas fuelled with both tritium and deuterium beams behaves as expected under fast ion diffusion modelling (Fig. 4). These plasmas have ~30% neutron emission from beam–beam reactions (Fig. 7(a)) and beam ion diffusion affects them the most. The beam–target neutrons also decrease with increasing D_f. The thermal neutrons increase somewhat with increasing D_f, but being only a minor part in the total neutron emission, do not affect its overall decrease.

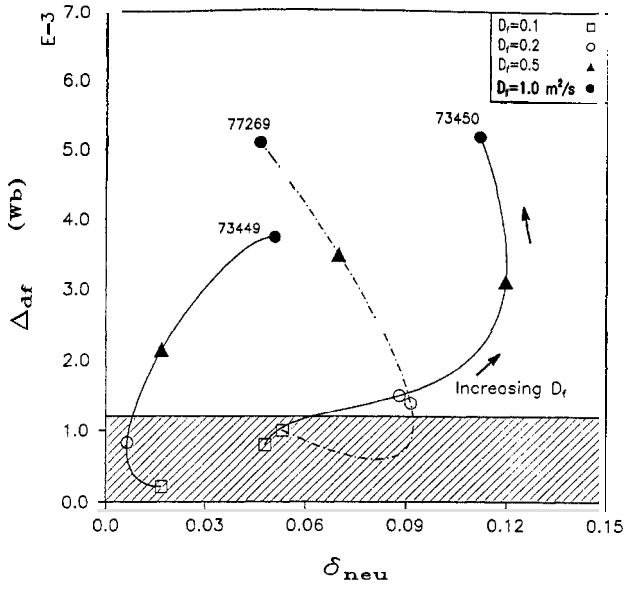

FIG. 10. Map showing the insensitivity of the total neutron emission for DT plasmas fuelled with pure deuterium (No. 73449) or pure tritium beams (Nos 73450, 77369).

5. CONCLUSIONS

We analyse a set of DD and DT plasmas for the effects of fast ion diffusion. The TRANSP predicted neutron emission and diamagnetic flux are compared with the baseline ($D_f = 0$) simulations, as well as with measurement. The results from plasmas heated with different fractions of deuterium and tritium beams, and power, and the systematic error analysis of one of these plasmas, establish a low value of the fast ion diffusion coefficient ($D_f \leq 0.2$ m^2/s). The long decay of the 14 MeV neutron emission from a short DT beam pulse sets an even lower limit: $D_f < 0.05$ m^2/s.

Both the neutron emission and the diamagnetic flux are mostly sensitive to the core beam ions. The low value of the fast ion diffusion coefficient in DT supershots is comparable with the values of the core thermal ion and electron heat diffusivities (~0.1 m^2/s) and confirms the excellent confinement properties of these plasmas.

Increased beam ion transport is observed in a DT plasma with large major and minor radius ($D_f \leq$ 0.3–0.4 m^2/s). The neutron emission and stored energy in a similar large, but low current, DD plasma imply substantial beam ion transport ($D_f > 1.0$ m^2/s).

There is no difference in diamagnetic flux sensitivity to fast ion diffusion modelling for DD and DT plasmas: it increases with beam power, and stored energy, for both of them. However, the neutron emission sensitivity *decreases* with beam power and stored energy (the L mode plasmas being particularly insensitive). For all plasmas, the larger the fraction of beam–beam neutrons, the more sensitive the neutron emission is. Plasmas fuelled with deuterium and tritium beams have less sensitive neutron emission if the tritium beam fraction is larger.

Wall recycling has a very strong effect in DT plasmas heated with pure tritium (deuterium) beams. These plasmas have small beam–beam, and large thermal neutron components, with the unusual final consequence that the TRANSP predicted total neutron emission does not change even for high values of D_f.

Fast ion loss experiments based on measurements of the plasma stored energy and total neutron emission have to consider the accuracy of those measurements, and the observed opposite sensitivities of the diamagnetic flux and neutron emission, with beam power. For DT plasmas, heating with one tritium beam line and three or four deuterium beam lines promises the most sensitivity of the neutron emission to fast ion diffusion.

In the course of our investigation of fast ion transport in TFTR plasmas we found evidence of spatially variable diffusion [32, 35]. Neutron flux measurements [30] indicate small D_f at the plasma centre, and increased D_f away from it. Therefore, the spatially constant D_f modelling we used is a limitation of this study. In future work, we will compare simulations that employ spatially dependent values of $D_f(r)$ with profile measurements of the neutron emission.

Systematic study of low beam power (< 10 MW) DD and DT plasmas, as well as plasmas with combined neutral beam and ICRF heating is desirable. When $P_{ICRF} \cong P_{NBI}$, most of the fast ion energy is in its perpendicular component and the diamagnetic flux is particularly sensitive to anomalous behaviour.

Finally, re-examination of the cases with suspected stochastic ripple loss is necessary. The newly installed stochastic ripple loss model in TRANSP is likely to clarify the nature of the observed enhanced fast ion transport in large TFTR plasmas. With such evidence at hand, and provided that the stochastic ripple loss is under control, good fast ion confinement in reactor-like DT plasmas is quite possible.

Appendix

SYSTEMATIC ERROR ANALYSIS OF SHOT 73457

Ideally, every plasma discharge from Section 3.2 should undergo random and systematic error analysis. However, that is a very expensive proposition:

a TRANSP simulation takes about 20 hours of CPU time on a DEC Alpha workstation (AXP 3000/300) and generates 30–40 MB data. The first check to drop is the random error analysis. Instead of generating an ensemble of simulations, each one with a random perturbation (within the corresponding error bars) of all the input data, and then looking at the distribution of the TRANSP predicted DMF and neutron emission, it is better to concentrate on systematic errors that are likely to have the most impact on the prediction of these two quantities. Second, we limit our investigation to a representative discharge from the DT plasma set.

TABLE II. SYSTEMATIC ERROR ANALYSIS OF SHOT 73 457

Baseline model	Thermal ion species independent transport model	
Trial number	Single variable/model changed	Changed by
1	B_t	+0.9%
2	Vis. Bremss.	+15%
3	Vis. Bremss.	−15%
4	Recycling	+100%
5	Recycling	−50%
6	Beam power	+3%
7	Beam power	−5%
8	n_e	+3%
9	n_e	−3%
10	T_e	+7%
11	T_e	−7%
12	T_i	$+T_{i(err)}$
13	T_i	$-T_{i(err)}$
14	$\sigma_{th,NBI}$	+60%
15	Z_{imp}	6.5→7.0
16	New full/half beam energy fractions	
17	Olson model for beam deposition on impurities	
18	Beam deposition on excited ion states	
19	Wall recycling fractions H, D, T changed to 10, 89.5, 0.5, resp.	
20	ECE T_e recalibrated to a TS T_e profile	
	Mixed thermal ion transport models	
21	$D_{th.(H,D,T)}$ = 1 m^2/s v_H:v_D:v_T = 1:1:1	
22	$D_{th.(H,D,T)}$ = 1 m^2/s v_H:v_D:v_T = 1:2:3	
23	$D_{th.(H,D,T)}$ = 1 m^2/s v_H:v_D:v_T = 3:2:1	
24	$D_{th.(H,D,T)}$ = 5 m^2/s v_H:v_D:v_T = 1:1:1	

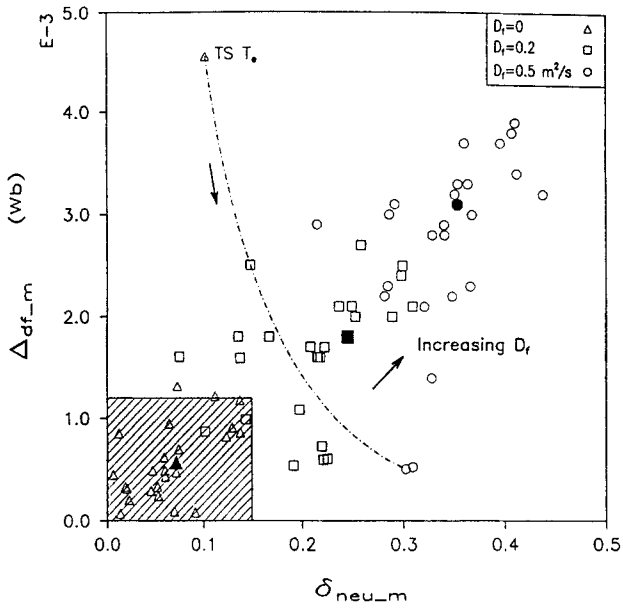

FIG. 11. Systematic error analysis map for shot No. 73457 (two tritium and six deuterium beams, P_{NBI} = 20 MW). The shaded box represents the boundaries of simulations within the experimental error bars. The filled symbols belong to a simulation that is tested against change in the input data or models (hollow symbols).

Two sources of systematic errors might bias the output of the TRANSP simulations. One is the possible systematic error in the input data, the other is the choice of physics models.

A single discharge (No. 73457) with good sensitivity to fast ion diffusion modelling is tested against various perturbations in the input data and a choice of beam deposition and thermal hydrogenic transport models. A set of simulations, each with one perturbed input data, or different model, is created (Table II). The resultant (δ_{neu_m}, Δ_{df_m}) measurement comparison map is given in Fig. 11.

All but two $D_f = 0$ predictions are within the measurement error. All simulations with $D_f = 0.5$ m^2/s substantially underestimate both the neutron emission and the diamagnetic flux, thus placing their (δ_{neu_m}, Δ_{df_m}) map points far away from the error-bar box. The map points from simulations with $D_f = 0.2$ m^2/s are placed in between, except for two cases. The point inside the box, close to its upper right corner, belongs to a simulation with the visible bremsstrahlung data reduced by 15%. The other point, further inside the box, belongs to the final test with simultaneous changes of several parameters (tests Nos 3, 5, 6 and 23). The goal of the final test is to

push the neutron emission, with each change, above the measured value.

The test that stands out in the map belongs to the simulation with electron temperature data recalibrated to a T_e profile from the 76 channel Thomson scattering (TS) diagnostics [36].

In the course of the TFTR DT experiments electron temperature is measured with a 20 channel grating polychromator [37] normalized to an absolutely calibrated Michelson interferometer [38]. Usually its profiles are narrower than those from the TS diagnostics and the central T_e is higher. Indeed, this is a case with shot 73 457: at 3.9 s, $T_e(0)$ is 25% higher than $T_e(0)$ from the TS diagnostics. The discrepancy between the two T_e diagnostics has been a matter of controversy at TFTR for the past few years. This time, our TRANSP simulations clearly question the validity of the Thomson scattering data. The dash-dotted line in Fig. 11 connects map points from $D_f = 0$, 0.2, 0.5 m^2/s simulations with the electron temperature recalibrated to the TS profile. The zero diffusion simulation predicts neutron emission within the ±15% error bar, but the diamagnetic flux is outside the 1.2 mWb error bar. Its stored energy increases 14% with respect to the baseline simulation (the simulation whose parameters are being perturbed). At first glance this contradicts the 25% lower central TS T_e, yet the much broader TS profile is responsible for a 30% increase of the electron stored energy. The parallel (perpendicular) beam ion energy increases 14% (17%) and the thermal ion stored energy decreases 7% from the baseline level. Another argument against the validity of the Thomson data is that the recalibrated profiles are hollow during most of the beam heating interval.

The baseline simulation, subsequently perturbed with a single change in the input data or model (Table II), assumes proportionality among the thermal hydrogen, deuterium and tritium ion density profiles ('thermal ion species independent transport model'). The same assumption is used in the time independent code SNAP [39–41]. By simultaneous solution of the quasi-neutrality and Z_{eff} equations, a common thermal hydrogenic profile is obtained. Then a fraction of this profile is assigned to each species, depending on the electron and beam ion density, limiter gas flow, etc.

Alternatively, each hydrogenic ion density can be set to evolve independently ('mixed model'). The radial fluxes are modelled with diffusive and convective terms:

$$\Gamma_\nu = D_\nu \nabla n_\nu + v_\nu n_\nu, \qquad \nu = \mathrm{H, D, T}$$

where D_ν and v_ν are spatially constant. Usually D_ν is kept constant for all three hydrogenic species. The values of the convective velocities cannot be explicitly set, because that would violate the simultaneous solution of the quasi-neutrality and the Z_{eff} equations. Instead, their ratio is specified.

Although the baseline simulation is in good agreement with the measured neutron emission and diamagnetic flux, the mixed thermal ion models improved the shape similarity between the TRANSP predicted and the measured data. A particularly good agreement was achieved in test No. 23 (Table II).

Simulations that did not change the neutron emission or DMF much include: the four tests with varied mixed thermal ion models (Nos 21–24), the test with increased impurity Z_{eff} (No. 15) and the test with altered recycling coefficients (No. 19). These coefficients are inferred from the relative intensities of the H_α, D_α and T_α spectral line emission at the plasma edge, viewed along five poloidal lines of sight [42]. The baseline simulation assumes 20% hydrogen, 77.5% deuterium and 2.5% tritium composition of the limiter influx.

Little change occurred when the old full/half neutral beam fractions (64%/28% for tritium, 45%/29% for deuterium) were substituted with the recently measured values (49%/38% for tritium, 43%/39% for deuterium). Use of the the old Olson model [43] for beam deposition on impurites instead of the new Phaneuf model [44], as well as the model with beam deposition on excited ion states [45] left the TRANSP predictions within 5% of the baseline simulation, which is also the TRANSP Monte Carlo noise level.

However, the ad hoc 60% increase in the thermal plasma stopping cross-section for beam ions only (test No. 14) had visible effects: the neutron emission and the stored energy dropped about 10%. The influence was even greater on the $D_f = 0.2$, 0.5 m^2/s simulations.

The 3% increase of the beam power had little effect on the simulations. The 5% decrease moved the corresponding $D_f = 0$ map point (not shown) in the middle of Fig. 11, thus simulations with $D_f > 0$ were not attempted, since they would produce map points further away from the error-bar box.

The impact of measurement error on electron density and ion temperature was also assessed. While the effect on the neutron emission is small, little (for n_e variations) to substantial effects (for T_i variations) on the diamagnetic flux were observed. In particular, the ±3% (this is the absolute error for the typical $n_e(0)$ values [46]) variation on n_e had a small effect on both

the neutron emission and the diamagnetic flux (Nos 8 and 9). The ±7% (one σ, Ref. [47]) variation on T_e had little effect on the neutron emission and a substantial effect on the plasma stored energy (Nos 10 and 11). The second zero diffusion map point on Fig. 11 that is outside the error-bar box, belongs to a simulation with T_e scaled down by 7%. The T_i measurement error is calculated for each of the 15 channels of the visible charge exchange recombination spectroscopy diagnostics [48] and is typically below 10% (one σ). The variation of the T_i profiles up and down from their nominal values had a particularly strong influence on the plasma stored energy in the $D_f > 0$ simulations (Nos 12 and 13). For example, use of the upper bound on the T_i measurement results in $D_f = 0.2$, 0.5 m^2/s predictions for the diamagnetic flux that are well within the 1.2 mWb error bar. Similar observation holds for the use of the upper bound on the T_e measurement.

Overall, the largest impact on the perturbed simulations was achieved with changes in the toroidal magnetic field (test No. 1), visible bremsstrahlung (tests Nos 2 and 3), recycling source strength (tests Nos 4 and 5) and electron and ion temperatures (tests Nos 10 to 13). To check the combined effect of perturbations that tend to increase the neutron emission, a final simulation was performed. It combined tests Nos 3, 5, 6 and 23. The resulting $D_f = 0.2$ m^2/s simulated neutron emission and diamagnetic flux lie within the diagnostic error bars.

ACKNOWLEDGEMENTS

We acknowledge the USDOE for support under Contract No. DE-FG03-92ER5415. We are especially grateful to D. McCune, Princeton Plasma Physics Laboratory, for sharing his knowledge of TRANSP. Helpful discussions with C.W. Barnes, M. Bell, S.D. Scott, J.D. Strachan and M.C. Zarnstorff, and the access to data measured by the TFTR team, are gratefully acknowledged.

REFERENCES

[1] PUTVINSKI, S., in Workshop on DT Experiments, Princeton, Vol. 2, PPPL, NJ (1994).
[2] ZWEBEN, S.J., et al., Nucl. Fusion **31** (1991) 2219.
[3] HEIDBRINK, W.W., SADLER, G.J., Nucl. Fusion **34** (1994) 535.
[4] SCOTT, S.D., et al., in Plasma Physics and Controlled Nuclear Fusion Research 1992 (Proc. 13th Int. Conf. Washington, DC, 1990), Vol. 1, IAEA, Vienna (1991) 235.
[5] CONROY, S., et al., in Controlled Fusion and Plasma Heating (Proc. 17th Eur. Conf. Amsterdam, 1990), Vol. 14B, Part I, European Physical Society, Geneva (1990) 98.
[6] DUONG, H.H., HEIDBRINK, W.W., Nucl. Fusion **33** (1993) 211.
[7] HAWRYLUK, R.J., et al., Plasma Phys. Control. Fusion **33** (1991) 1509.
[8] COTTRELL, G.A., START, D.F.H., Nucl. Fusion **31** (1991) 61.
[9] STRACHAN, J.D., et al., Nucl. Fusion **21** (1981) 67.
[10] JET TEAM, Nucl. Fusion **32** (1992) 187.
[11] HAWRYLUK, R.J., in Physics of Plasmas Close to Thermonuclear Conditions (Proc. Course Varenna, 1979), Vol. 1, CEC, Brussels (1980) 19.
[12] GOLDSTON, R.J., in Basic Physical Processes of Toroidal Fusion Plasmas (Proc. Course and Workshop Varenna, 1985), Vol. 1, CEC, Brussels (1986) 165.
[13] ZARNSTORFF, M.C., et al., Phys. Fluids B **2** (1990) 1852.
[14] RUSKOV, E., et al., Bull. Am. Phys. Soc. (1993) 2036.
[15] McCUNE, D., Princeton Plasma Physics Laboratory, NJ, personal communication, 1994.
[16] BUDNY, R.V., et al., Nucl. Fusion **32** (1992) 429.
[17] WIELAND, R.M., et al., Rev. Sci. Instrum. **59** (1988) 1768.
[18] NIESCHMIDT, E.B., et al., Rev. Sci. Instrum. **56** (1985) 1084.
[19] HENDEL, H.W., IEEE Trans. Nucl. Sci. **NS-39** (1986) 670.
[20] HENDEL, H.W., et al., Rev. Sci. Instrum. **59** (1988) 1682.
[21] HENDEL, H.W., et al., Rev. Sci. Instrum. **61** (1990) 1900.
[22] BARNES, C.W., et al., Rev. Sci. Instrum. **61** (1990) 3151.
[23] JOHNSON, L.C., et al., Rev. Sci. Instrum. **66** (1995) 894.
[24] JASSBY, D.L., et al., Rev. Sci. Instrum. **66** (1995) 891.
[25] RUSKOV, E., et al., Rev. Sci. Instrum. **66** (1995) 910.
[26] BARNES, C.W., et al., Rev. Sci. Instrum. **61** (1990) 3190.
[27] COONROD, J., et al., Rev. Sci. Instrum. **56** (1985) 941.
[28] BELL, M.G., et al., Plasma Phys. Control. Fusion **28** (1986) 1329.
[29] BELL, M., Princeton Plasma Physics Laboratory, NJ, personal communication, 1994.
[30] ROQUEMORE, A.L., et al., Rev. Sci. Instrum. **61** (1990) 3163.
[31] STRACHAN, J.D., et al., Phys. Rev. Lett. **58** (1987) 1004.
[32] HEIDBRINK, W.W., et al., Phys. Fluids B **3** (1991) 3167.
[33] PETRASSO, R., Nature **369** (1994) 105.
[34] BUDNY, R.V., TFTR GROUP, J. Nucl. Mater. **176&177** (1990) 427.
[35] RUSKOV, E., et al., in Workshop on DT Experiments, Princeton, Vol. 2, PPPL, NJ (1994).
[36] JOHNSON, D., et al., Rev. Sci. Instrum. **56** (1985) 1015.
[37] CAVALLO, A., et al., Rev. Sci. Instrum. **59** (1988) 889.
[38] STAUFFER, F.J., et al., Rev. Sci. Instrum. **59** (1988) 2139.
[39] TOWNER, H.H., et al., Rev. Sci. Instrum. **63** (1992) 4753.
[40] MURPHY, J.A., et al., The SNAP User's Guide, Rep. PPPL-TM-393, PPPL, NJ (1992).
[41] MURPHY, J.A., et al., Rev. Sci. Instrum. **63** (1992) 4750.
[42] RAMSEY, A.T., TURNER, S.L., Rev. Sci. Instrum. **58** (1987) 1211.

[43] OLSON, R.E., et al., Phys. Rev. Lett. **41** (1978) 163.
[44] PHANEUF, R.A., et al., Collisions of Carbon and Oxygen Ions with Electrons, H, H_2, and He, Rep. ORNL-6090/V5, ORNL, TN (1987).
[45] JANEV, R.K., et al., Nucl. Fusion **29** (1989) 2125.
[46] PARK, H.K., Rev. Sci. Instrum. **61** (1990) 2879.
[47] TAYLOR, G., Princeton Plasma Physics Laboratory, NJ, personal communication, 1994.
[48] STRATTON, B.C., et al., in Time Resolved Two- and Three-Dimensional Plasma Diagnostics (Proc. IAEA Tech. Comm. Mtg Nagoya, 1990), IAEA, Vienna (1990) 78.

(Manuscript received 2 December 1994
Final manuscript accepted 23 March 1995)